Indian Journal of Science and Technology, *Vol 8(26), DOI: 10.17485/ijst/2015/v8i26/80457, October 2015*
ISSN (Print) : 0974-6846
ISSN (Online) : 0974-5645

Control of Chaotic Resonance Phenomena using Prototypes in Manifold Forms

Jeongho Cho[1], Dong-Gi Kwag[2*] and Byung-Seo Kim[3]

[1]Department of Avionics Engineering, Hanseo University, Taean-gun - 357-953, Korea; jcho@hanseo.ac.kr
[2]Department of Aeromechanical Engineering, Hanseo University, Taean-gun - 357-953, Korea; dgkwag@hanseo.ac.kr
[3]Department of Computer and Information Communication Engineering, Hongik University, Sejong City - 339-701, Korea

Abstract

This paper presents a modeling strategy using prototypes in manifold forms for unknown chaotic behaviors, observed possibly in power electronics, robot manipulators, lasers, etc.; it models from only a finite number of one dimensional time series observables in order to simplify both the modeling and the controller design. With the intention of dividing the operating space into a set of smaller regions, the Self-Organizing Map (SOM) is employed as a modeling groundwork and prototypes in manifold forms attached to the SOM are created in the least square sense for each region. Once a set of prototypes representing the operating space is established, the regional controllers associated with the prototypes are designed with a traditional PID control law. Switching of the controllers is done synchronously by the SOM, which chooses the regional operating space, linked with an active regional prototype valid in a certain operating regime. Simulations on the chaotic oscillator regulating the unknown chaos to a fixed point or a stable periodic orbit illustrate the efficiency of the proposed modeling and control architecture.

Keywords: Chaotic Resonance, Modeling, PID Control, Self-Organizing Map

1. Introduction

Modeling and control of nonlinear dynamical systems is of great practical significance and, in particular, controlling chaos observed in wide areas such as lasers and plasma technologies, mechanical and chemical systems, power electronics, robotics, telecommunications, system automations, etc., has become interesting and received more special attention since the dynamic behaviors of chaotic systems are very complicated and challenging even though their model descriptions are relatively simple. Mostly, a typical structure for control of the chaotic systems is based upon an exact chaotic model. For the case when the system is unknown, however, the controller design needs to be started with an attempt to derive a model capable of controlling the underlying chaotic dynamics[1–3,11,12].

In particular, the idea of local modeling has been an area of interest in modeling and controller design in order to simplify them[4,5]. Local modeling is to identify a nonlinear system with a set of local models representing each operating regions. If a nonlinear system f to be modeled is complicated, it may not be capable of approximating f equally well across all operating space. In this case, the dependence on representation can be reduced using local approximation where the domain of f is decomposed into regional domains and a separate model is used for each region[5,6,13].

For the decomposition of the domain of f, a Self-Organizing Map (SOM) has been employed to divide the operating region into local zones. The SOM is particularly appropriate for switching, because it converts complex, nonlinear statistical relationships of high-dimensional data into uncomplicated geometric connections that preserve the topology in the feature

**Author for correspondence*

space[7]. Thus the role of the SOM is to discover shapes in the high dimensional state space and divide it into a set of areas represented by the weights of each Processing Element (PE). Under some mild conditions, it has been shown that a suit of local models can uniformly approximate any system on a closed subset of the state space provided a sufficient number of local models are given[5,6].

While classical control techniques have produced many highly reliable and effective control systems, the PID control methodology has been extensively studied by researchers and well understood by practitioners. Most of PID controllers proposed in the literature, however, have been developed mainly based on the state-space model under the assumption that all state variables are measurable or on the input-output model for a linear system[8]. Furthermore, a typical PID control scheme cannot be extended to nonlinear systems and thus we exploit prototypes in manifold forms with switching to approximate the nonlinear dynamics in order to avoid such difficulty.

The prototypes in manifold forms based control structure proposed in this paper is rooted in the principle of using regional models to construct a globally nonlinear model, when pieced together, that is determined completely from the input-output observables[5,14]. The prototypes in manifold forms are selected and derived through competition using the SOM and they are built from the data samples corresponding to each PE of the SOM. Associated prototype-based local controllers are designed by means of using any standard linear PID controller design method and it only needs to determine the desired controller coefficients based on each prototype selected.

In summary, the aim of this paper is to illustrate how a modeling strategy using prototypes in manifold forms can be incorporated with the well-known linear PID controller design techniques to obtain a principled and simple nonlinear PID controller design approach. Simulation results on a Duffing chaotic oscillator, assuming that no a priori knowledge about the system is available, are presented to demonstrate the effectiveness of the proposed methodology in modeling, controlling and synchronizing.

2. Preliminaries on Local Modeling

A general nonlinear system can be described as follows:

$$\begin{aligned} \dot{x}(t) &= g(x(t), u(t), t) \\ y(t) &= h(x(t), t), \end{aligned} \tag{1}$$

where $x(t) \in \Re^l$ is the system state vector at time t; $u(t) \in \Re^l$ is a given control action; and $g : \Re^{2l+1} \to \Re^l$ is an unknown nonlinear function describing the dynamics of a system. In case we have to determine a model from a finite number of measurements of the system's input-output observables, a nonlinear dynamic system, g, can be described by a NARX (Nonlinear Auto-Regressive with exogenous input) model that is an extension of a linear ARX model[4], and represents the system by a nonlinear connection of past input and output terms to future output, that is,

$$y_k = f(y_{k-1}, \cdots, y_{k-m}, u_{k-1}, \cdots, u_{k-n}), \tag{2}$$

where $y_k \in Y \subset \Re^p$ is the output vector and $u_k \in U \subset \Re^q$ is the input vector. For simplicity, setting $p = q = 1$ and let the $(m+n)$ - dimensional basis vector be

$$\vec{\psi}_k = [\vec{\psi}_k^y, \vec{\psi}_k^u]^T = [y_{k-1}, \cdots, y_{k-m}, u_{k-1}, \cdots, u_{k-n}]^T, \tag{3}$$

where $\vec{\psi}_k$ is in the set $\Psi = Y^m \times U^n$. If the nonlinear function f is invertible *w.r.t.* the input u_k, then a controller may be constructed easily. However, unfortunately, most nonlinear functions are not invertible, so the application of this approach is limited. Thus it is tempting to use a modeling framework using prototypes in manifold forms which approximate a nonlinear function, f, with a set of relatively simple local models valid in certain operating regions such that the whole operating space is decomposed into very simple linear models switched[5,6]. The underlying dynamics f in (2) is then approximated as $f \approx \bigcup_{i=1}^{N} \{f_i\}$ where N is the number of operating spaces. Provided that necessary smoothness conditions on $f_i : \Psi \to Y$ are satisfied, a Taylor series expansion can be used around the operating point[6]. The first-order approximation about the system's equilibrium point produces N local predictive ARX models $f_1, \cdots, f_N$ of the plant described by

$$f_i(\vec{\psi}_k) \approx \sum_{j=1}^{m} a_{i,j} y_{k-j} + \sum_{j=1}^{n} b_{i,j} u_{k-j}, \quad i = 1, \cdots, N, \tag{4}$$

where $a_{i,j}$ and $b_{i,j}$ are the parameters of the i^{th} model. The parameters $\{a_{i,j}, b_{i,j}\}$ are subsequently estimated from the selected pairs $\{y_{k-j}, u_{k-j}\}$ on the local operating regime in the least square sense.

In this way of approximation of an autonomous system, local linear models have performed very well in comparative studies on time series prediction problems and in most cases have generated more accurate predictions than global methods[4,5].

3. Modeling Strategy using Prototypes in Manifold Forms

To devise a reasonable identification strategy for controlling unknown chaotic systems, the idea of local modeling is employed in such a way that the systems are approximated by means of a set of relatively simple Prototypes in Manifold Forms (PMF) valid in certain conditions. The SOM is utilized as a modeling infrastructure to construct PMF. It provides a codebook representation of the system dynamics and organizes the different dynamic regimes in topological neighborhoods. This feature of the SOM can facilitate to create a set of prototypes that are local to the data in the Voronoi tessellation created by the SOM[5,7].

The SOM is trained to resemble the input space and position the local prototypes. Let the delayed output vector, $\vec{\psi}_k^y$, be the input to the SOM, and the synaptic weight vector, $\vec{w}_i, i \in \{1, \cdots, L\}$, of each PE i in the SOM have the same dimension of the input space. To find the best match of the input vector $\vec{\psi}_k^y$ with the weight vector $\vec{w}_i$, the Euclidean distance between $\vec{\psi}_k^y$ and each $\vec{w}_i$ is computed. Then the index of the PE with the smallest distance is selected as $i^o = \underset{1 \le i \le N}{argmin} \left\| \vec{\psi}_k^y - \vec{w}_i \right\|$, which summarizes the essence of the competition process among the PEs. The particular PE that satisfies this condition is called the winning PE, i^o, for the input vector, $\vec{\psi}_k^y$. The winning PE locates the center of a topological neighborhood of cooperating PEs. The weight vector $\vec{w}_i$ of each PE is then updated as

$$\vec{w}_{i,k+1} \leftarrow \vec{w}_{i,k} + \bullet_k \Lambda_{i,k} (\vec{\psi}_k^y - \vec{w}_{i,k}), \tag{5}$$

where $\eta_k \in [0,\ 1]$ is the learning rate to control the speed of convergence; $\Lambda_{i^o,i}$ is the topological neighborhood function centered on the winning PE i^o, and is typically defined as $\Lambda_{i^o,i,k} = exp\left(-\left\| r_i - r_{i^o} \right\|^2 / 2\sigma_k^2 \right)$, where $\left\| r_i - r_{i^o} \right\|$ represents the Euclidean distance in the output lattice between the i^{th} PE and the winning PE and σ_k is the effective width of the topological neighborhood. Notice that both the learning rate, η_k, and the neighborhood width, σ_k, are time dependent and normally annealed to provide the best performance with the least training time[5].

Once the SOM is suited to preserve topological relationships in the input space, the available data is partitioned into smaller sets; the samples associated with the weight vector $\vec{w}_i$ are $\left\{ \vec{\psi}_{i,1}^y, \cdots, \vec{\psi}_{i,N_i}^y \right\}$, where N_i is the number of samples clustered to PE i. Then, each PE is extended with a local prototype incorporated with the delayed version of control input $\vec{\psi}_k^u$; it can be optimized using the least squares with this input-output training data that is clustered to this PE in the SOM so that $\hat{y}_k = f_i(\vec{\psi}_k^y, \vec{\psi}_k^u)$.

4. Controller Design for Prototypes in Manifold Forms

Once system identification is complete, the design of a globally Prototypes in Manifold Forms based Control (PMFC) structure can be easily accomplished using standard PID control techniques. The literature has an abundance of PID design methodologies for linear Single-Input Single-Output (SISO) systems including direct pole-placement techniques and optimal coefficient adjustment according to some criteria. Here pole-placement technique[8] is utilized to design a PID controller for each linear SISO prototype and is illustrated briefly in the following.

Assume that the plant is approximated by a set of the SISO, second-order system given by

$$y_{k+1} = f_i(y_k, y_{k-1}, u_k, u_{k-1}) = a_{1,i} y_k + a_{2,i} y_{k-1} + b_{1,i} u_k + b_{2,i} u_{k-1}, \tag{6}$$

where is y_k the output of the plant and u_k is the input to the plant. Each prototype's transfer function is given by

$$F_i(q^{-1}) = \frac{B_i(q^{-1})}{A_i(q^{-1})} = \frac{b_{1,i} + b_{2,i} q^{-1}}{1 - a_{1,i} q^{-1} - a_{2,i} q^{-2}}. \tag{7}$$

It is assumed that the polynomials $A_i(q^{-1})$ and $B_i(q^{-1})$ do not have any common factors. Note that in order to have a stable zero, $b_{1,i} > b_{2,i}$ must be true. The controller is then designed by starting with a general PID regulator represented by $G_i(q^{-1}) = D_i(q^{-1}) / C_i(q^{-1})$, and determining the coefficients of polynomials C_i and D_i so that the closed-loop system has desired properties. The goal of the controller design is thus to map the values of $\{a_{1,i}, a_{2,i}, b_{1,i}, b_{2,i}\}$ into the controller coefficients $\{c_{l,i}, d_{m,i}\}$, subject to the constraint of the prototype whose characteristic polynomial is $1 + \lambda_1 q^{-1} + \lambda_2 q^{-2}$. The characteristic polynomial of the closed-loop system is $A_i(q^{-1}) C_i(q^{-1}) + q^{-1} B_i(q^{-1}) D_i(q^{-1})$ and simplifying and equating characteristic polynomials results in the design equation

$$A_i(q^{-1})(1 - q^{-1})(1 - c_i q^{-1}) + q^{-1} B_i(q^{-1}) D_i(q^{-1}) = A_o(q^{-1}) A_m(q^{-1}), \tag{8}$$

where the characteristic polynomial for the model is $A_m(q^{-1}) = 1 + \lambda_1 q^{-1} + \lambda_2 q^{-2}$, with the addition of a second-order "observer polynomial" term $A_o(q^{-1}) = q^{-2}$. This equation is solved for $\{c_i, d_{m,i}\}$ and consequently the control law is determined as

$$u_k = (1-c_i)u_{k-1} + c_i u_{k-2} + d_{1,i}e_k + d_{2,i}e_{k-1} + d_{3,i}e_{k-2}, \quad (9)$$

of the i^{th} controller.

Given the PMFs as obtained through the use of a SOM and a PID controller design technique, the overall closed-loop nonlinear PID design reduces to determining the coefficients of the individual local linear PID controllers using their associated respective linear prototypes. One needs to determine a set of PID coefficients per prototype. In the competitive SOM approach, the overall system output depends only on a single prototype at a given time; therefore, the PID coefficients are set to those values determined for the instantaneous winning prototype.

5. Simulation Results

To examine the effectiveness of the proposed modeling architecture using PMF and controller design strategy, a Duffing oscillator was considered assuming that its nonlinear dynamics f is completely unknown and there exists the only state available for measurement. The oscillator considered displays chaotic behavior described by

$$\begin{aligned} \dot{x}_1 &= x_2 \\ \dot{x}_2 &= u - p_1 x_2 - p_2 x_1 - p_3 x_1^3 + p_4 \cos \omega t, \end{aligned} \quad (10)$$

where ω is a constant frequency parameter, p_1, p_2, p_3 and p_4 are constant parameters [3].

We assumed that only measurable quantity is $y = x_1$ and the controlled Duffing oscillator is originally (u = 0) in the chaotic state, as shown in Figure 1, with parameters $\omega = 1.8$, $[p_1, p_2, p_3, p_4] = [0.4, -1.1, 1.0, 1.8]^T$. In the simulations, we generated time-series data excited by zero-mean and unit variance perturbation, via the fourth-order Runge-Kutta scheme with a fixed time step of 0.2. The number of delay taps for reconstruction of the input space was chosen as $m = 2$ and $n = 2$ based on the Lipschitz index[9] exhibited in Figure 2 and a set of prototypes was accordingly constructed as $\hat{y}_k = f_i(y_{k-1}, y_{k-2}, u_{k-1}, u_{k-2})$.

Then the SOM was trained over 6,000 samples with the time decaying parameters, $\eta_k = 0.1/(1+0.003k)$

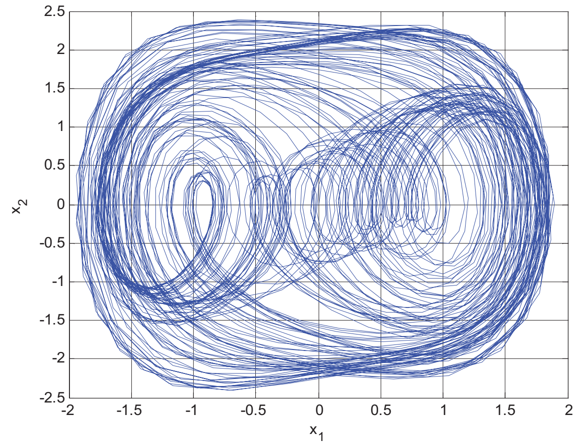

Figure 1. The phase-space trajectory of uncontrolled Duffing oscillator.

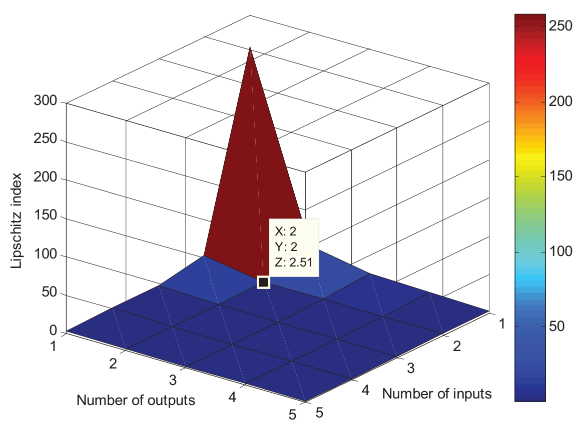

Figure 2. Lipschitz index for the determination of optimal number of inputs and outputs.

and $\sigma_k = (\sqrt{N}/2)/(1+0.003k)$ and a newly generated sequence of 1,000 samples was applied to the PMF for the test. Another parameter to be selected is the size of the SOM which is trained with $\vec{\psi}_k^y = [y_{k-1}, y_{k-2}]^T$. We chose the number of PEs (N) in the SOM as 4×4 based on the generalization error as seen in Figure 3 since the modeling performance evaluated by Signal-to-Error Ratio (*SER*), defined in $SER[dB] = 10 \cdot \log_{10}\left\{\sum_k y_k^2 \Big/ \sum_k (y_k - \hat{y}_k)^2\right\}$, was not improved much after $\sqrt{N} = 4$.

The identification result with 4×4 square map, 16 PMFs in total, is demonstrated in Figure 4 and its performance comparisons with one of global models, Time Delay Neural Network (TDNN)[10] which is very suitable to create a model and a controller when only input-output measurements are available, as well as a single ARX model are also presented in Table 1. We observe that the proposed modeling strategy is a very good approximation of the controlled Duffing oscillator and outperforms both a linear and a nonlinear global modeling paradigm. It also should be noted that the proposed modeling scheme makes the system identification very computationally efficient because chaotic dynamics are captured in a compact lookup table of prototypes.

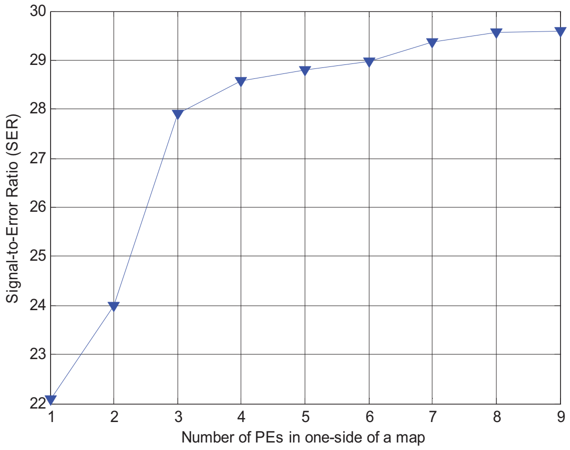

Figure 3. SER v.s. Number of PEs in one-side of a map.

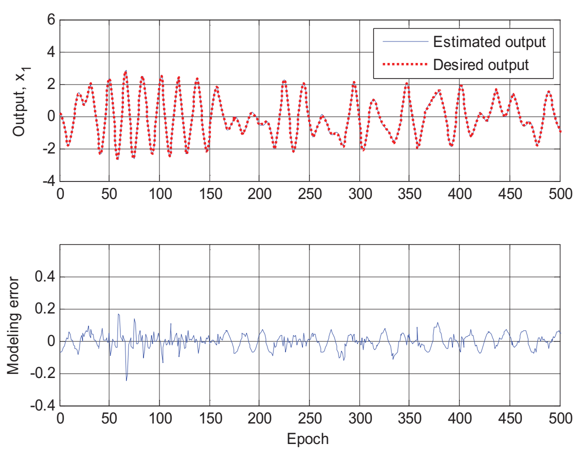

Figure 4. Modeling performance of the controlled Duffing oscillator by PMF

Table 1. Comparison of modeling performance for the controlled duffing oscillator

Methodology	*SER [dB]*
ARX (1)	23.92
PMF (16)	28.50
TDNN (4:14:1)	26.40

Next, we carried out simulations for 3 different control tasks using the created PMFs.

1. Control of the Duffing oscillator to approach a static point, which is $x_1 = 0$, $x_2 = 0$.
2. Control of the Duffing oscillator trajectory to a periodic orbit, which is the period-1 orbit of the oscillator created by using $\omega = 1.8$, $[p_1, p_2, p_3, p_4] = [0.4, -1.1, 1.0, 0.62]^T$
3. Synchronization of two strictly different second order oscillators in spite of model mismatch; the master oscillator is a van der Pol one which is described by $\dot{x}_1 = x_2,\ \dot{x}_2 = -0.1(x_1^2 - 1)x_2 - x_1^3 + 1.75\cos(0.667t)$.

For these missions, the optimal number of PEs in the hidden layer of the TDNN Controller (TDNNC) was selected as 30 by 20 Monte-Carlo simulations and the PMFC were designed for placing the poles of the closed-loop response at $0.2 \pm i0.2$ which demonstrated the fastest convergence of the desired trajectory.

We then compared the performance of the controllers using 150 epoch-long oscillatory trajectory regarding a settling time and a root mean squared steady-state error in Table 2; the settling time was selected when the tracking error was bounded in ± 0.1 and the steady-state error was calculated using the tracking error from 100 to 150 epochs. Each controller was activated after an epoch of 51. As seen in the table, the proposed PMFC is more suitable in tracking of an unknown chaotic system than a global controller, TDNNC, which is generally utilized for unknown system control, in both fast response and accuracy.

Figures 5–7 show comparison results in terms of tracking control by the TDNNC and the PMFC. It is demonstrated that, in all the control tasks, the transient time is significantly shortened without resulting in overshoots using the PMFC. Especially, while the TDNNC demonstrated some difficulty in following the desired path generated from a different dynamics, the van der Pol oscillator, the PMFC accomplished the mission relatively well.

Table 2. Comparison of tracking performance in terms of a transient time (Epoch) and a steady-state error for 3 different tasks

Methodology	Task 1	Task 2	Task 3
PMFC	3 / 2.2e-3	8 / 1.8e-3	8 / 1.1e-3
TDNNC	21 / 5.7e-3	14 / 6.6e-3	44 / 4.8e-3

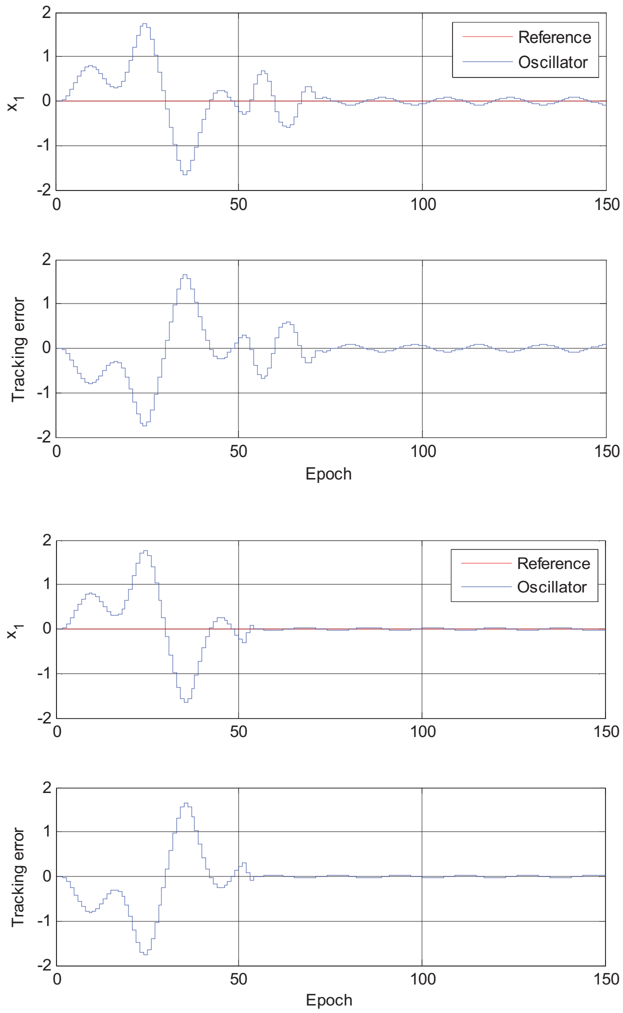

Figure 5. Comparison of a static point tracking performance by TDNNC (top) and PMFC (bottom).

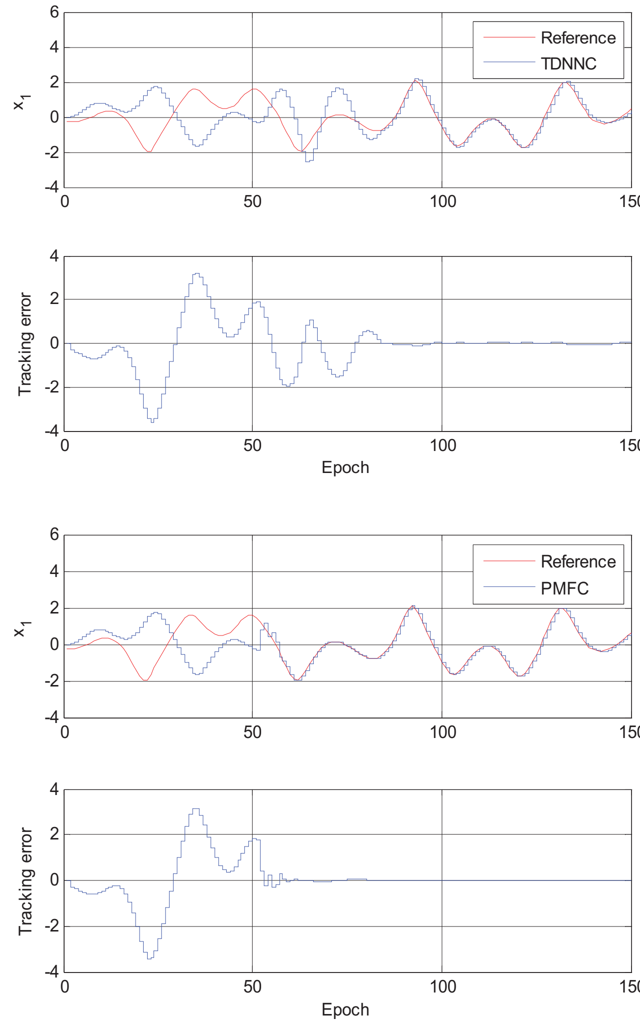

Figure 7. Comparison of synchronization performance by TDNNC (top) and PMFC (bottom).

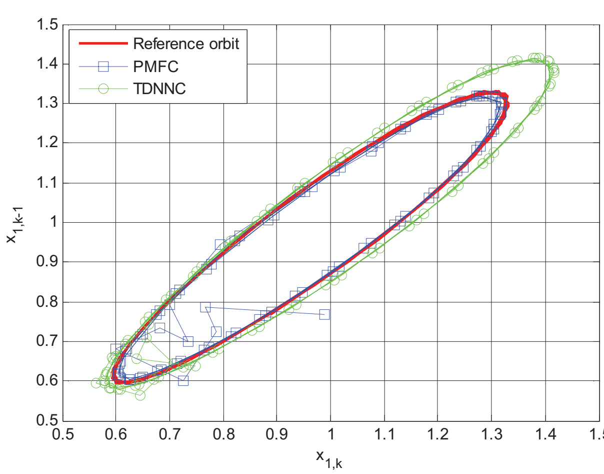

Figure 6. Comparison of a periodic orbit tracking performance by TDNNC and PMFC.

6. Concluding Remarks

In this paper, we have proposed exploiting the locally linear nature of nonlinear dynamical systems in their state space resulting in the PMFs which adopts the divide-and-conquer type strategy. In this regard, the concept of self-organization was taken in the output space extended with the PMFs by the SOM for system identification. By adaptively determining the optimal locations for placing the PMFs and training individual prototypes with appropriately selected input-output observables, a piece-wise linear approximation of the global nonlinear dynamics was obtained even in the cases where the state variables are not available or accessible.

This approximation allowed us to employ well-established linear PID controller design techniques for the local prototypes, yet still achieve a globally nonlinear PID control scheme. Simulation results, forcing the output observable to asymptotically track the reference signal without any a priori knowledge of the Duffing oscillator, showed that the derived control fashion using the PMFs is highly promising and easy to implement by demonstrating that it outperforms a traditional globally adaptive nonlinear controller, TDNNC.

7. References

1. Poznyak AS, Yu W, Sanchez EN. Identification and control of unknown chaotic systems via Dynamic Neural Networks. IEEE Trans Cir and Sys-I. 1999 Dec; 46(12):1491–5.
2. Chen G, Chen G, Figueiredo RJP. Feedback control of unknown chaotic dynamical systems based on time-series data. IEEE Trans Circuits and Systems-I. 1999 May; 46(5):640–4.
3. Ge SS, Wang C, Lee TH. Adaptive backstepping control of a class of chaotic systems. Int J Bifurcation and Chaos. 2000 May; 10(5):1149–56.
4. Murray-Smith R, Johansen TA. Multiple model approaches to modeling and control. Taylor and Francis Inc; 1997.
5. Principe JC, Wang L, Motter MA. Local dynamic modeling with self-organizing maps and applications to nonlinear system identification and control. Proceedings of the IEEE. 1998 Nov; 86(11):2240–58.
6. Farmer JD, Sidorowich JJ. Predicting chaotic time series. Phys Rev Let. 1987 Aug; 59(8):845–8.
7. Kohonen T. Self-Organizing Maps. Springer; 1995.
8. Brown RE, Maliotis GN, Gibby JA. PID self-tuning controller for aluminum rolling mill. IEEE Trans Industry Applications. 1993 May/Jun; 29(3):578–83.
9. He X, Asada H. A new method for identifying orders of input-output models for nonlinear dynamic systems. Proc American Control Conference. San Francisco, CA, USA. 1993 Jun 2-4; p. 2520–3.
10. Nguyen DH, Widrow B. Neural Networks for self-learning control systems. IEEE Trans Control Systems Magazine. 1990 Apr; 10(3):18–23.
11. Gritli H, Belghith S, Khraief N. OGY-based control of chaos in semi-passive dynamic walking of a torso-driven biped robot. Nonlinear Dyn. 2015 Jan; 79(2):1363–84.
12. Moreno-Valenzuela J. Adaptive anti control of chaos for robot manipulators with experimental evaluations. Comm Nonlinear Sci Numer Simulat. 2013 Jan; 18(1):1–11.
13. Meng Q, Peng Y. A new local linear prediction model for chaotic time series. Physics Letters A. 2007 Oct; 370(5-6):465–70.
14. Garcia-Nieto S, Martinez M, Blasco X, Sanchis J. Nonlinear predictive control based on local model networks for air management in diesel engines. Control Eng Practice. 2008 Dec; 16(12):1399–413.